Least squares method to solve 3D convection–diffusion–reaction equation with variable coefficients in multi-connected domains

E. C. ROMÃO[1] and L. F. M. MOURA[2]

[1]*Federal University of Itajubá – Advanced Campus of Itabira, Itabira/MG, Brazil.* [2]*Thermal and Fluids Engineering Department, Mechanical Engineering Faculty, State University of Campinas, Campinas/SP, Brazil*
** Correspondence: E. C. Romão. E-mail: estaner23@yahoo.com.br or estanerromao@unifei.edu.br.*

Abstract - This paper aims at analyzing 3D convection-diffusion-reaction in multi-connected domains. The objective is to create two types of domains (double and multi-connected), to analyze the influence of numerical results for the proposed methods (GFEM and LSFEM). The domain and the construction of the networks proposed in this paper are applications built with the aim of facilitating the comparison of works by other researchers.

Keywords – convection-diffusion-reaction problems, GFEM, LSFEM, multi-connected domains.

1 Introduction

In [1] a study of three-dimensional diffusion-reaction in the form of the equation

$$k_x \frac{\partial^2 T}{\partial x^2} + k_y \frac{\partial^2 T}{\partial y^2} + k_z \frac{\partial^2 T}{\partial z^2} + BT = 0 \tag{1}$$

with k_x, k_y and k_z constant, $B = B(x,y,z)$ e $T = T(x,y,z)$ are functions of the spatial coordinates x, y and $z \in \mathbb{R}$ is accomplished through two applications: first solving the Poisson equation (pure diffusion) and the second the Helmholtz equation (diffusion-reaction). In this work, these two applications will be dealt with, but with a new configuration in the domain. In the diffusion reaction, a hole (double convex domain) is inserted, and in the pure diffusion, two holes (multi-connected domain). The two holes configuration will be used to analyze a problem proposed in [2], which deals with issues of convection-diffusion-reaction with variable coefficients in the form of the equation

$$k_x \frac{\partial^2 T}{\partial x^2} + k_y \frac{\partial^2 T}{\partial y^2} + k_z \frac{\partial^2 T}{\partial z^2} + A_x \frac{\partial T}{\partial x} + A_y \frac{\partial T}{\partial y} + A_z \frac{\partial T}{\partial z} + BT = 0 \tag{2}$$

with k_x, k_y and k_z constant, $B = B(x,y,z)$, $A_x = A_x(x,y,z)$, $A_y = A_y(x,y,z)$, $A_z = A_z(x,y,z)$ and $T = T(x,y,z)$ are functions of the spatial coordinates x, y and $z \in \mathbb{R}$. For this comparison, the application 6 of [2] will be used, where the convection coefficients vary quadratically with the spatial coordinates. Finally, a new convection-diffusion with analytical solution application will be proposed and analyzed with a configuration containing two holes.

2 Formulation

Here is a summary of the formulation according to the Galerkin and Least Squares methods. It will use the equation (2) that represents the three phenomena: convection, diffusion and reaction.

2.1 Least Squares

When applying the least squares method used for three-dimensional phenomena, the addition of three auxiliary equations, will generate a system of four differential equations of the first order with four variables, defined as follows,

$$k_x \frac{\partial q_x}{\partial x} + k_y \frac{\partial q_y}{\partial y} + k_z \frac{\partial q_z}{\partial y} + A_x \frac{\partial T}{\partial x} + A_y \frac{\partial T}{\partial y} + A_z \frac{\partial T}{\partial z} + BT = 0\,, \tag{3a}$$

$$q_x - \frac{\partial T}{\partial x} = 0\,, \tag{3b}$$

$$q_y - \frac{\partial T}{\partial y} = 0\,, \tag{3c}$$

$$q_z - \frac{\partial T}{\partial z} = 0 . \tag{3d}$$

Note that the three equations auxiliary, equations (3b-d) have immediately returned, the numeric result of the derivatives of temperature in the three spatial coordinates.

The least squares method generates a linear system in the form [3]:

$$\begin{bmatrix} A & B & C & D \\ B^T & E & G & H \\ C^T & G^T & I & J \\ D^T & H^T & J^T & K \end{bmatrix} \begin{Bmatrix} \hat{T}^e \\ \hat{q}_x^e \\ \hat{q}_y^e \\ \hat{q}_z^e \end{Bmatrix} = \begin{bmatrix} 0 \\ 0 \\ 0 \\ 0 \end{bmatrix}, \tag{4}$$

where:

$$A_{ij} = \int_{\Omega^e} \left\{ \left[A_x \frac{\partial N_i}{\partial x} + A_y \frac{\partial N_i}{\partial y} + A_z \frac{\partial N_i}{\partial z} + BN_i \right] \times \left[A_x \frac{\partial N_j}{\partial x} + A_y \frac{\partial N_j}{\partial y} + A_z \frac{\partial N_j}{\partial z} + BN_j \right] + \frac{\partial N_i}{\partial x}\frac{\partial N_j}{\partial x} + \frac{\partial N_i}{\partial y}\frac{\partial N_j}{\partial y} + \frac{\partial N_i}{\partial z}\frac{\partial N_j}{\partial z} \right\} d\Omega , \tag{5a}$$

$$B_{ij} = \int_{\Omega^e} \left\{ \left[A_x \frac{\partial N_i}{\partial x} + A_y \frac{\partial N_i}{\partial y} + \alpha A_z \frac{\partial N_i}{\partial z} + BN_i \right] \times \left[k_x \frac{\partial N_j}{\partial x} \right] - \frac{\partial N_i}{\partial x} N_j \right\} d\Omega , \tag{5b}$$

$$C_{ij} = \int_{\Omega^e} \left\{ \left[A_x \frac{\partial N_i}{\partial x} + A_y \frac{\partial N_i}{\partial y} + A_z \frac{\partial N_i}{\partial z} + BN_i \right] \times \left[k_y \frac{\partial N_j}{\partial y} \right] - \frac{\partial N_i}{\partial y} N_j \right\} d\Omega , \tag{5c}$$

$$D_{ij} = \int_{\Omega^e} \left\{ \left[A_x \frac{\partial N_i}{\partial x} + A_y \frac{\partial N_i}{\partial y} + A_z \frac{\partial N_i}{\partial z} + BN_i \right] \times \left[k_z \frac{\partial N_j}{\partial z} \right] - \frac{\partial N_i}{\partial z} N_j \right\} d\Omega , \tag{5d}$$

$$E_{ij} = \int_{\Omega^e} \left[k_x^2 \frac{\partial N_i}{\partial x}\frac{\partial N_j}{\partial x} + N_i N_j \right] d\Omega , \tag{5e}$$

$$G_{ij} = \int_{\Omega^e} k_x k_y \frac{\partial N_i}{\partial x}\frac{\partial N_j}{\partial y} d\Omega , \tag{5f}$$

$$H_{ij} = \int_{\Omega^e} k_x k_z \frac{\partial N_i}{\partial x}\frac{\partial N_j}{\partial z} d\Omega , \tag{5g}$$

$$I_{ij} = \int_{\Omega^e} \left[k_y^2 \frac{\partial N_i}{\partial y}\frac{\partial N_j}{\partial y} + N_i N_j \right] d\Omega , \tag{5h}$$

$$J_{ij} = \int_{\Omega^e} k_y k_z \frac{\partial N_i}{\partial y}\frac{\partial N_j}{\partial z} d\Omega , \tag{5i}$$

$$K_{ij} = \int_{\Omega^e} \left[k_z^2 \frac{\partial N_i}{\partial z}\frac{\partial N_j}{\partial z} + N_i N_j \right] d\Omega . \tag{5j}$$

Significantly, the formulation of the problem posed by the LSFEM follows that the system described in (4) is symmetrical and positive-definite for any of the equation's coefficients values (2). Furthermore, there is the advantage of holding only the non-null coefficients from the global matrix, these being of type $i \geq j$, i.e., only the coefficients of the upwards main diagonal, because of the matrix symmetry. Note that for the GFEM this is only possible for non-convective issues, which can be seen next in the Eq. (10a). Further details of this formulation can be found in [2].

2.2 The Galerkin Method

Taking as residual the following equation,

$$R = k_x \frac{\partial^2 T}{\partial x^2} + k_y \frac{\partial^2 T}{\partial y^2} + k_z \frac{\partial^2 T}{\partial z^2} + A_x \frac{\partial T}{\partial x} + A_y \frac{\partial T}{\partial y} + A_z \frac{\partial T}{\partial z} + BT , \tag{6}$$

And replacing it, in equation [4,5],

$$\int_{\Omega^e} R \, v_i^e d\Omega = 0 , \ \forall v_i^e \in V^e , \ i = 1,2,..., N_{Nnodes} \tag{7}$$

where N_{nodes} is the number of nodes in element.

The following is the integral element,

$$\int_{\Omega^e} \left[k_x \frac{\partial^2 T}{\partial x^2} + k_y \frac{\partial^2 T}{\partial y^2} + k_z \frac{\partial^2 T}{\partial z^2} + A_x \frac{\partial T}{\partial x} + A_y \frac{\partial T}{\partial y} + A_z \frac{\partial T}{\partial z} + BT \right] N_j d\Omega = 0 . \tag{8}$$

The application of some integration techniques and some algebraic equations generates the following linear system,

$$[K]\{T_i^e\} = \{F\}, \tag{9}$$

in which

$$K_{ij} = -\int_{\Omega^e} k_x \frac{\partial N_i}{\partial x}\frac{\partial N_j}{\partial x} d\Omega - \int_{\Omega^e} k_y \frac{\partial N_i}{\partial y}\frac{\partial N_j}{\partial y} d\Omega - \int_{\Omega^e} k_z \frac{\partial N_i}{\partial z}\frac{\partial N_j}{\partial z} d\Omega + \int_{\Omega^e} BN_i N_j d\Omega + \int_{\Omega^e} A_x \frac{\partial N_i}{\partial x} N_j d\Omega + \int_{\Omega^e} A_y \frac{\partial N_i}{\partial y} N_j d\Omega + \int_{\Omega^e} A_z \frac{\partial N_i}{\partial z} N_j d\Omega , \quad (10a)$$

$$F_i = \int_{\Gamma_q} N_j (q + h(T - T_a)) d\Gamma_q . \quad (10b)$$

Where Γ represents the contour, h is the heat transfer coefficient, T_a is the environmental temperature, and q is the contour's heat flux density.

Unlike the LSFEM, in the GFEM for the calculation of the temperature's derivatives in the three spatial coordinates, an artifice of some kind will be necessary to calculate the derivatives from the values found in $T(x, y, z)$. The alternative used in this work, will be to calculate them by approximation provided as follows,

$$\frac{\partial T}{\partial x_k} \approx \frac{\partial \hat{T}^e}{\partial x_k} = \sum_{i=1}^{Nnodes} \frac{\partial N_i}{\partial x_k} \hat{T}_i^e ,$$

Where k = 1, 2 or 3, where $x_1 = x$, $x_2 = y$ and $x_3 = z$.

3 Numerical Applications

The calculation of the matrix coefficients (4), and (9) are obtained by the Gauss numerical integration [4], with the actual elements mapping through the reference elements in the local coordinates ξ, η and ζ ($-1 \le \xi,\eta,\zeta \le 1$), where the Lagrange interpolation functions will be used [5].

The systems of algebraic equations represented in (9) for GFEM, and in (4) for the LSFEM will be solved by the Gauss-Seidel methodology, and with the stopping criterion with a maximum error of $E_{max} \le 10^{-10}$. The computer code was developed in Fortran language, on a computer with the following characteristics: Intel Corel 2 Duo, 2, 19 GHz, 8GB de RAM. The networks were internally generated for the Cartesian domains. The actual elements are taken as straight prisms and they are refined within the limits of the computer's available memory. As mentioned earlier, the domains and the adopted networks were chosen to facilitate the comparison of results by other researchers.

To analyze the results of the four applications that will be proposed in this paper, because of the existing analytical solution for them, the contour conditions are adopted to meet the analytical solution. For the analysis of error in the numerical solution will be used two types of norms; the L_2 norm of error defined in [6] as $\|e\| = \left[\left(\sum_{i=1}^{Nnost} e_i^2\right) / Nnost\right]^{1/2}$, with *Nnost* as the number of nodes across the network, and $e_i = T_{(num)i} - T_{(an)i}$, where $T_{(num)}$ is the numerical solution result and $T_{(an)}$ the result of the analytical solution. This norm aims to provide a notion of the average error committed in the entire analyzed domain.

In addition to the L_2, the L_∞ norm defined as: $e_i = | T_{(num)_i} - T_{(an)_i} |$ will be used as well. The L_∞ norm represents the largest network error for each type of refinement.

In the following applications is assumed that $h = \Delta x = \Delta y = \Delta z$, where Δx, Δy, e Δz the hexahedron edges. As shown in [1,2], the networks will be built, for the posed problems, with linear hexahedrons (with linear interpolation functions - 8 nodes) which are already presenting very good results.

Application 1 - Diffusion-Reaction

This application will be adopting an analytical solution for equation (2), with k_x, k_y, k_z and B units, as follows,

$$T(x, y, z) = \sin x + \sin y + \sin z$$
$$\frac{\partial T(x, y, z)}{\partial x} = \cos x ,$$
$$\frac{\partial T(x, y, z)}{\partial y} = \cos y , \frac{\partial T(x, y, z)}{\partial z} = \cos z .$$

Furthermore, it will be used a configuration with one hole. The construction was performed from a straight-rectangle parallelepiped, measuring $0 \le x, z \le 1$ and $0 \le y \le 0.5$ with a hole inserted through the *xz* face, as shown in Fig 1.

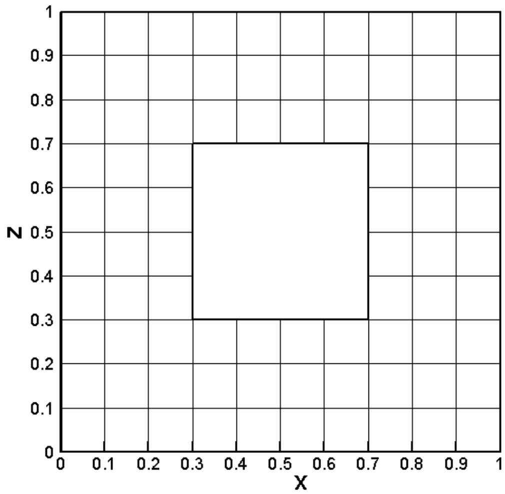

Fig. 1 Network with a hole, the *xz* plane vision

Comparing the numerical results from Tables 1 to 3 with the results shown in application 2 in [1]. It is noted that the overall order of precision found in the two cases are similar; demonstrating that the two methods provided excellent results for the solution of $T(x,y,z)$ (in the order of 10^{-6} for an $h = 1/10$) even with the existence of a hole in the domain. In the event of a hole, one must consider the existence of contour conditions, not only on the outside of the cube but also on the inside (hole). Again, the LSFEM showed about 2-3 orders of precision better than the GFEM (Tables 2 and 3). Table 2 shows the numerical results of $\partial T/\partial x$ and $\partial T/\partial z$, the differences were insignificant to the point of being considered as equals in this work.

Table 1 Results for the solution of $T(x,y,z)$, application 1

NNost	Nelem*	h	L₂ norm		L∞ norm	
			Galerkin	LSFEM	Galerkin	LSFEM
672	420	1/10	4.85E-06	5.74E-06	1.58E-05	2.34E-05
4312	3360	1/20	1.33E-06	1.60E-06	4.01E-06	5.94E-06
13440	11340	1/30	6.40E-07	7.45E-07	1.91E-06	2.66E-06

**Nelem*: number of elements in the computational network.

Table 2 Results for the solution of $T_x(x,y,z) = T_z(x,y,z)$, application 1

h	L_2 norm		L_∞ norm	
	Galerkin	LSFEM	Galerkin	LSFEM
1/10	2.57E-02	6.15E-05	4.12E-02	2.05E-04
1/20	1.30E-02	1.88E-05	2.08E-02	7.05E-05
1/30	8.72E-03	1.33E-05	1.39E-02	9.77E-05

Table 3 Results for the solution of $T_y(x,y,z)$, application 1

h	L_2 norm		L_∞ norm	
	Galerkin	LSFEM	Galerkin	LSFEM
1/10	1.34E-02	1.59E-05	2.26E-02	5.16E-05
1/20	6.87E-03	4.74E-06	1.16E-02	1.95E-05
1/30	4.61E-03	5.24E-06	7.84E-03	4.01E-05

Application 2 - Pure Diffusion

This application will adopt an analytical solution for Eq. (2), with k_x, k_y, k_z unitary and B null, as follows,

$$T(x,y,z)=\frac{\sin(\pi.y)\sin(\pi.z)}{\sinh(\pi\sqrt{2})}\times \left[2\sinh(\pi\sqrt{2}x)+\sinh(\pi\sqrt{2}(1-x))\right],$$

$$\frac{\partial T(x,y,z)}{\partial x}=\frac{\sin(\pi.y)\sin(\pi.z)}{\sinh(\pi\sqrt{2})}\times \left[2\sqrt{2}\pi\cosh(\pi\sqrt{2}x)-\sqrt{2}\pi\cosh(\pi\sqrt{2}(1-x))\right],$$

$$\frac{\partial T(x,y,z)}{\partial y}=\frac{\pi\cos(\pi.y)\sin(\pi.z)}{\sinh(\pi\sqrt{2})}\times \left[2\sinh(\pi\sqrt{2}x)+\sinh(\pi\sqrt{2}(1-x))\right],$$

$$\frac{\partial T(x,y,z)}{\partial z}=\frac{\sin(\pi.y)\pi\cos(\pi.z)}{\sinh(\pi\sqrt{2})}\times \left[2\sinh(\pi\sqrt{2}x)+\sinh(\pi\sqrt{2}(1-x))\right].$$

Now, contrary to the first application, it will be adopted a multi-connected domain, where a straight-rectangle parallelepiped identical to the first application, but with two holes instead of one, as shown in Figure 2, is used as computational domain.

When comparing the numerical results exhibited in Tables 4-6; with the results from the unitary cube domain shown in application 1 [1], it is noted that the order of precision is even better with the existence of two holes. This can be demonstrated, e.g., for an h = 1/10 in the $T(x,y,z)$ solution, where the order of precision for a network with two holes is in the order of 10^{-4}, while for the unitary cube is in the order of 10^{-3} to the L_2 norm. Essentially, the results displayed in Table 4 show that the three proposed refinements demonstrate little difference of precision; therefore, it is not advisable, in this case, a further refining of the network, because with a h = 1/10 network, an actual error in the order of 10^{-4} for temperature analysis issues; is considered outstanding. As in the case of the unitary cube [1], the GFEM showed the worst results in the temperature variation analysis in the three spatial directions. Again, the LSFEM displayed better results in this analysis; thus, demonstrating its potential application for calculating heat fluxes.

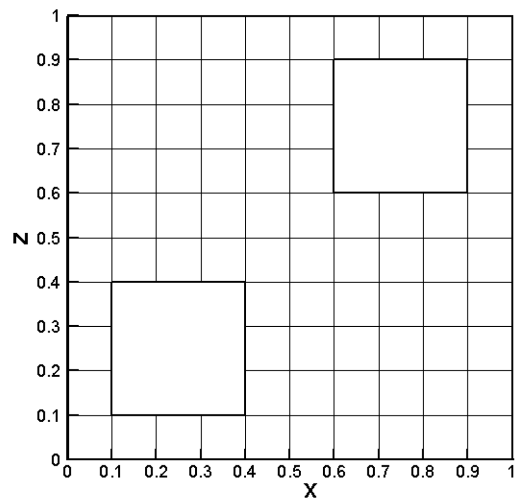

Fig. 2 Network with two holes, the *xz* plane vision

Table 4 Results for the solution of $T(x,y,z)$, application 2

NNost	Nelem	***h***	**L_2 norm**		**L_∞ norm**	
			Galerkin	**LSFEM**	**Galerkin**	**LSFEM**
678	410	1/10	8.88E-04	9.13E-04	3.97E-03	4.59E-03
4301	3280	1/20	2.43E-04	2.46E-04	9.68E-04	1.15E-03
13328	11070	1/30	1.12E-04	1.13E-04	4.28E-04	5.08E-04

Table 5 Results for the solution of $T_x(x,y,z)$, application 2

h	**L_2 norm**		**L_∞ norm**	
	Galerkin	**LSFEM**	**Galerkin**	**LSFEM**
1/10	3.91E-01	1.48E-02	1.71E-00	1.16E-01
1/20	1.97E-01	7.65E-03	9.18E-01	4.58E-02
1/30	1.31E-01	4.69E-03	6.27E-01	2.43E-02

Table 6 Results for the solution of $T_y(x,y,z) \cong T_z(x,y,z)$, application 2

h	**L_2 norm**		**L_∞ norm**	
	Galerkin	**LSFEM**	**Galerkin**	**LSFEM**
1/10	2.14E-01	6.42E-03	9.78E-01	4.21E-02
1/20	1.00E-01	4.29E-03	4.92E-01	3.45E-02
1/30	6.78E-02	2.72E-03	3.28E-01	1.88E-02

Application 3 - Diffusion-Convection

In this application, a case of convection-diffusion will be treated. Since there is no record, in the literature, for such an analytical solution, we proposed the following,

$$-\frac{\partial^2 T}{\partial x^2}-\frac{\partial^2 T}{\partial y^2}-\frac{\partial^2 T}{\partial z^2}+3\frac{\partial T}{\partial y}=0$$

With $T(x,y,z)=e^x e^y e^z$. Since, this is a one-way velocity problem (y direction), for a configuration containing the same network/domain from the earlier application (two holes), the assumption is of a constant velocity in the domain not influenced by the two holes.

Table 7, shows both methods having excellent results in the $T(x,y,z)$ solution; yet, in the temperature derivatives solution (Table 8), there is a significant decrease in the GFEM precision, with a reduction of four orders of precision compared to the one by the LSFEM. In other words, the LSFEM can virtually maintain the same precision for each of the adopted networks, either in the temperature solution or in the derivatives thereof.

This problem would be analogous to a Freon flow (Refrigerant-12) (CCI_2F_2), where for a temperature near 280K (note that for the analytic solution adopted, the temperature ranges varies from 274.15 K (1°C) to 285.33K (12.18°C in $(x,y,z)=(1,0.5,1)$) the thermal conductivity equals k = 0.073 W/mK, requiring a y-direction velocity of 0.219 m/s [7].

Table 7 Results for the solution of $T(x,y,z)$, application 3

h	**L_2 norm**		**L_∞ norm**	
	Galerkin	**LSFEM**	**Galerkin**	**LSFEM**
1/10	5.56E-05	5.48E-05	1.68E-04	1.64E-04
1/20	1.52E-05	1.49E-05	4.16E-05	4.18E-05
1/30	7.09E-06	6.87E-06	1.85E-05	1.87E-05

Table 8 Results the solution of $T_x(x,y,z) \cong T_y(x,y,z) \cong T_z(x,y,z)$, application 3

h	L_2 norm		L_∞ norm	
	Galerkin	LSFEM	Galerkin	LSFEM
1/10	2.11E-01	1.29E-04	5.89E-01	7.82E-04
1/20	1.04E-01	1.14E-04	2.99E-01	1.05E-03
1/30	6.93E-02	6.44E-05	2.00E-01	4.78E-04

Application 4 - Convection-Diffusion-Reaction with variable coefficients (quadratic functions)

As shown in [2], application 6, is proposed here a problem of convection-diffusion-reaction with variable coefficients according to the equation below,

$$\frac{\partial^2 T}{\partial x^2}+\frac{\partial^2 T}{\partial y^2}+\frac{\partial^2 T}{\partial z^2}+100(-x^2+x)\frac{\partial T}{\partial x}+ 100(-y^2+y)\frac{\partial T}{\partial y}+100(-z^2+z)\frac{\partial T}{\partial z}-BT=0$$

with $B=100[(-x^2+x)+(-y^2+y)+(-z^2+z)]+3$, in which the proposed analytical solution is of type $T(x,y,z)=e^{x+y+z}$.

As in the two previous applications, this will also employ the computational domain configuration shown in Figure 2. Essentially, the variable coefficients are used here to simulate a situation of variable velocity in three directions at all points of the network, not that these situations will necessarily become actual engineering issues.

Unlike the application 6 of [2], for a unitary cube, the numerical solution of $T(x,y,z)$ for the GFEM shows a decrease of nearly two orders of precision in the two holes case, while the LSFEM increased one (Table 9). Both methods have approximately the same orders of precision for the refinements adopted; however, the LSFEM was more efficient for the multi-connected domain than for the unitary cube, and the opposite occurred with the GFEM. In turn, the numerical precision of the derivatives in the temperature three directions (Table 10), in this configuration is similar to that presented in [2], emphasizing that the LSFEM in this application was incapable of assuring the same order of precision for the temperature solution.

4 Conclusions

The finite elements method has proven, over the years, to be a major tool in solving engineering problems involving heat and mass transfer, and of fluid mechanics. Some methods prove to be ineffective in situations more complex, where the domains are shown with irregularities, orifices and obstructions. Here, we show that the finite element method in the LSFEM and the GFEM variants, even for more complex cases, remains an excellent tool. In general, the two methods provided excellent results. In particular, the GFEM remains superior for the temperature analysis alone; while the LSFEM is outstanding for when the temperature and the heat flux are to be calculated, where the order of precision for the temperature and for the derivatives are equivalent.

Acknowledgments

The National Council of Scientific Development and Technology, CNPq, Brazil (Proc. 500382/2011-5) supported the present work.

Table 9 Results for the solution of $T(x,y,z)$, application 3

h	**L_2 norm**		**L_∞ norm**	
	Galerkin	**LSFEM**	**Galerkin**	**LSFEM**
1/10	4.55E-03	8.44E-03	1.30E-02	3.58E-02
1/20	1.36E-03	4.08E-03	3.55E-03	1.75E-02
1/30	6.49E-04	2.60E-03	1.64E-03	1.01E-02

Table 10 Results for the solution of $T_x(x,y,z) \cong T_y(x,y,z) \cong T_z(x,y,z)$, application 3

h	**L_2 norm**		**L_∞ norm**	
	Galerkin	**LSFEM**	**Galerkin**	**LSFEM**
1/10	2.09E-01	1.60E-01	5.89E-01	8.22E-01
1/20	1.03E-01	5.89E-02	2.99E-01	2.37E-01
1/30	6.88E-02	3.36E-02	2.00E-01	1.20E-01

References

[1] E. C. Romão, M. D. Campos, L. F. M. Moura, Application of Galerkin and Least-Squares finite element method in the solution of 3D Poisson and Helmholtz equations, *Computers & Mathematics with Applications*, vol. 62, 2011, p. 4288-4299.

[2] E. C. Romão, L. F. M. Moura, Galerkin and least squares method to solve 3D convection–diffusion–reaction equation with variable coefficients. *Numerical Heat Transfer, Part A – Applications*, 61, 2012, p. 669-698.

[3] B. N. Jiang, *The Least-Squares Finite Element Method: Theory and Aplications in Computational Fluid Dynamics and Electromagnetics*, Springer, New York, 1998.

[4] J. N. Reddy, *An Introduction to the Finite Element Method*, McGraw-Hill, New York, 1993.

[5] G. Dhatt, G. Touzot, *The Finite Element Method Displayed*. John Wiley and Sons, Chichester, 1978.

[6] M. Zlhmal, *Superconvergence and reduced integration in the finite element method*, *Math. and Comput.*. vol. 32, n. 143, 1978, p. 663-685.

[7] F. P. Incropera,, D. P. DeWitt, *Fundamentals of Heat and Mass Transfer*, Fifth Edition. John Wiley & Sons, Inc, 2003.